

Decoherence enhances performance of quantum walks applied to graph isomorphism testing

M. Bruderer and M. B. Plenio

Institut für Theoretische Physik, Albert-Einstein Allee 11, Universität Ulm, 89069 Ulm, Germany

(Dated: November 22, 2016)

Computational advantages gained by quantum algorithms rely largely on the coherence of quantum devices and are generally compromised by decoherence. As an exception, we present a quantum algorithm for graph isomorphism testing whose performance is optimal when operating in the partially coherent regime, as opposed to the extremes of fully coherent or classical regimes. The algorithm builds on continuous-time quantum stochastic walks (QSWs) on graphs and the algorithmic performance is quantified by the distinguishing power (DIP) between non-isomorphic graphs. The QSW explores the entire graph and acquires information about the underlying structure, which is extracted by monitoring stochastic jumps across an auxiliary edge. The resulting counting statistics of stochastic jumps is used to identify the spectrum of the dynamical generator of the QSW, serving as a novel graph invariant, based on which non-isomorphic graphs are distinguished. We provide specific examples of non-isomorphic graphs that are only distinguishable by QSWs in the presence of decoherence.

I. INTRODUCTION

The main objective of quantum information processing is to enhance the computational performance of quantum devices over comparable classical devices by exploiting coherent quantum effects. Incoherent or even dissipative processes therefore generally pose major obstacles to physical implementations of quantum computing [1]. That being said, it is known that incoherent effects can be utilized to accomplish specific tasks such as entanglement generation [2–4] and quantum teleportation [5]. Another example for beneficial effects of decoherence is dephasing-enhanced transport found in systems as diverse as light-harvesting complexes [6, 7], structured waveguide arrays [8], one-dimensional conductors [9] and arrays of quantum dots [10]. At the level of quantum algorithms for specific mathematical problems, however, it seems to be an established paradigm that algorithms relying on purely coherent quantum dynamics always outperform partially decoherent approaches [11, 12]. As a rare counterexample, algorithmic applications of decoherence have been reported in the context of quantum walks [13, 14].

In this paper we present a quantum algorithm whose performance is optimal when operating in the partially coherent regime and thus benefits from decoherence. The algorithm solves instances of a clearly defined mathematical task, namely the graph isomorphism (GI) problem [15]. The GI problem is central to graph theory and consists of testing if two graphs are isomorphic, i.e., if one graph can be mapped to the other by a relabeling of vertices. As of today, no efficient (polynomial-time) algorithm for the GI problem is known in full generality. However, for the vast majority of graphs, the problem can be solved efficiently in practice [16], and it has been recently shown that the GI problem can be solved in quasipolynomial-time in the worst case [17].

Here we consider a physically motivated approach towards solving the GI problem for certain classes of graphs. As often for GI testing, the performance of the algorithm is quantified by the distinguishing power (DIP) between non-isomorphic graphs, in contrast to runtime efficiency. The proposed algorithm for GI testing is formulated in terms of continuous-time quantum stochastic walks (QSWs) on graphs, whose dynamics spans the entire range between fully coherent quantum

walks and classical random walks [18]. QSWs allow us to study the workings of our algorithm under decoherence and to explore its quantum-to-classical transition. Similar to the results in Refs. [13, 14], we find that already a small amount of decoherence enhances the performance of our quantum algorithm.

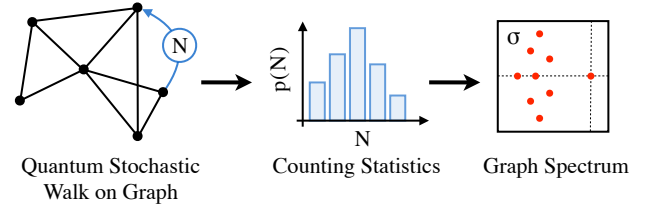


FIG. 1. Proposed algorithm for graph isomorphism testing: A quantum stochastic walk (QSW) on the graph relaxes to the steady state. The number of jumps N per time interval across an auxiliary edge is monitored, yielding the counting statistics $p(N)$. The distribution $p(N)$ is used to determine the complex spectrum σ of the generator of the QSW. Graphs are compared by their spectra, where different spectra indicate non-isomorphism.

The GI problem enjoys renewed popularity and several quantum (or quantum-inspired) algorithms for GI testing have been presented recently. As shown in Ref. [19], absorption spectra of exciton Hamiltonians with graph-structured interactions can be used to distinguish graphs. Algorithms for GI testing based on multi-particle quantum walks, relying on comparisons between evolution operators or occupation probabilities, have been proposed in Refs. [20–24], where the DIP depends on modifications of local phases and whether the evolution is discrete or continuous in time [25, 26]. Ideas originating from quantum walks have also been adapted to design classical algorithms for the GI problem [27, 28]. Apart from their theoretical appeal, both discrete- and continuous-time quantum walks have been experimentally implemented on various physical platforms, including NMR systems [29], trapped ions [30, 31] and photonic implementations [32–34].

Our algorithm is conceptually different from existing approaches in that both the initialization and readout are continuous processes. GI testing is achieved with the desired precision by continuously monitoring local fluctuations of QSWs

on the level of random trajectories, described by the counting statistics of stochastic jumps [35, 36]. Another feature is that, in the tradition of spectral graph theory [37, 38], the complex spectrum of the dynamical generator of the QSW serves as a graph invariant. In addition to its use as part of our quantum algorithm, this novel graph invariant may also serve as the basis for quantum-inspired algorithms.

Figure 1 illustrates the essential steps of the algorithm: For the initialization, an auxiliary edge is connected to two arbitrary vertices of the graph and the QSW is allowed to relax to the steady state. Subsequently, a counting device monitors stochastic jumps of the QSW across the auxiliary edge. During this continuous readout process, information about the graph structure is accumulated and encoded in the counting statistics $p(N)$ of the number of jumps N per time interval. Finally, the information contained in the distribution $p(N)$ is used to determine the spectrum σ of the generator of the QSW (as defined later). Isomorphism of two graphs G and G' is tested by comparison of their spectra σ and σ' , where different spectra imply non-isomorphic graphs.

The individual steps of the algorithm are explained in the rest of the paper. After preliminaries about graphs, we initially focus on the generator of the QSW as a matrix representation for graphs and analyze the spectrum of the generator for different levels of decoherence.

II. GRAPH INVARIANTS FROM QUANTUM STOCHASTIC WALKS

We consider undirected graphs $G = (V, E)$ consisting of the vertex set V and edge set E , where $(i, j) \in E$ denotes an edge between vertices $i, j \in V$ and $n = |V|$ is the number of vertices. The graphs are connected with neither multiple edges nor self-loops. The graph structure is encoded in the adjacency matrix A , with entries $A_{ij} = 1$ if $(i, j) \in E$ and $A_{ij} = 0$ otherwise, or described by the Laplacian matrix $L = D - A$. The degree matrix D with entries $D_{ii} = d_i$ is diagonal, where the degree d_i is the number of edges connected to vertex i . Other common matrix representations are the signless Laplacian $|L| = D + A$ and the adjacency matrix of the complement $\bar{A} = \mathbb{J} - A - \mathbb{1}$, with $\mathbb{1}$ the identity and \mathbb{J} the all-ones matrix. The GI problem in terms of matrix representations is equivalent to deciding if two adjacency matrices A and A' represent isomorphic graphs, i.e., whether or not there exists a permutation matrix Π such that $A = \Pi^{-1} A' \Pi$ holds.

An important concept of GI testing are graph invariants, defined as quantities $I(G)$ such that $I(G) = I(G')$ if G and G' are isomorphic [16, 39]. Graph invariants can be constructed through matrix representations M of graphs, where M stands for A , L or other representations. Important invariants are the characteristic polynomial $P^M(\mu) = \det[\mu\mathbb{1} - M]$ and the spectrum σ^M consisting of the roots of $P^M(\mu)$. We denote σ^M as M -spectrum and call two graphs M -cospectral if their M -spectra coincide. The coefficients of $P^M(\mu)$ are directly related to cycles and spanning trees of graphs [37], and the majority of graphs are identifiable by a single spectrum or combinations of different spectra [40–42].

We now turn to the generator of QSWs, which is an alternative matrix representation of the graph G , and discuss the corresponding graph invariants. QSWs on graphs account for both stochastic jumps and quantum tunneling between connected vertices [18]. For ensemble averages over trajectories, QSWs are described by an $n \times n$ density matrix ρ whose time evolution is governed by the quantum master equation

$$\frac{d\rho(t)}{dt} = \mathcal{L}^\omega \rho(t) = [\omega \mathcal{L}^{\text{qm}} + (1 - \omega) \mathcal{L}^{\text{cl}}] \rho(t). \quad (1)$$

The generator \mathcal{L}^ω is decomposed into \mathcal{L}^{qm} and \mathcal{L}^{cl} such that the coherence $\omega \in [0, 1]$ parametrizes the quantum-to-classical transition. In terms of quantum walks under decoherence the parameter $1 - \omega$ quantifies the strength of adverse environmental effects. The generator \mathcal{L}^{qm} of the coherent dynamics acts on the density matrix as $\mathcal{L}^{\text{qm}} \rho = -i[A, \rho]$ and the generator \mathcal{L}^{cl} of the classical dynamics is the Lindblad dissipator

$$\mathcal{L}^{\text{cl}} \rho = \sum_{i,j} A_{ij} \left(\Upsilon_{ij} \rho \Upsilon_{ij}^\dagger - \frac{1}{2} \{ \Upsilon_{ij}^\dagger \Upsilon_{ij}, \rho \} \right), \quad (2)$$

where the operators $\Upsilon_{ij} = |j\rangle\langle i|$ map state $|i\rangle$ to $|j\rangle$. The dissipator \mathcal{L}^{cl} induces stochastic jumps between vertices and is closely related to the Laplacian L , the generator of classical random walks [43]. Dephasing operators $\Upsilon_{ii} = |i\rangle\langle i|$ are not contained in \mathcal{L}^{cl} since $A_{ii} = 0$; however, dephasing terms occur for graphs with self-loops.

The generator \mathcal{L}^ω is a matrix representation in the same sense as the adjacency matrix A . As a linear superoperator in Liouville space, \mathcal{L}^ω is represented by an $n^2 \times n^2$ matrix in the dyadic basis $\{|i\rangle\langle j|\}$ (with $i, j = 1, \dots, n$) acting on the vector ρ with n^2 components. In this representation we obtain explicit expressions for the characteristic polynomial $P^\omega(\nu) = \det[\nu\mathbb{1} - \mathcal{L}^\omega]$ and the spectrum $\sigma^\omega = \{\nu_1, \dots, \nu_{n^2}\}$. The eigenvalues ν_i are either real-valued or come in complex conjugate pairs such that $P^\omega(\nu) = \nu^{n^2} + q_{n^2-1}\nu^{n^2-1} + \dots + q_1\nu + q_0$ has real coefficients q_i . For a detailed understanding of the spectrum of \mathcal{L}^ω (ω -spectrum for short) as a graph invariant we consider the extreme limits $\omega = \{0, 1\}$, thereby relating the ω -spectrum to the spectrum of the adjacency and Laplacian matrix.

The generator \mathcal{L}^{cl} of the classical random walk ($\omega = 0$) is applied to basis vectors $\{|i\rangle\langle j|\}$ to determine its structure. Considering separately occupations $|i\rangle\langle i|$ and coherences $|i\rangle\langle j|$ with $i \neq j$ we obtain

$$\begin{aligned} \mathcal{L}^{\text{cl}} |i\rangle\langle i| &= \sum_{\ell} A_{i\ell} |\ell\rangle\langle \ell| - d_i |i\rangle\langle i|, \\ \mathcal{L}^{\text{cl}} |i\rangle\langle j| &= -\frac{1}{2} (d_i + d_j) |i\rangle\langle j|. \end{aligned} \quad (3)$$

Equations (3) show that \mathcal{L}^{cl} does not mix occupations and coherences, and is therefore block diagonal in the basis $\{|i\rangle\langle j|\}$. The block acting on occupations, in matrix form, is identical to the negative of the Laplacian L , whereas the coherences are eigenvectors of \mathcal{L}^{cl} with eigenvalues $-\frac{1}{2}(d_i + d_j)$. The spectrum $\sigma^{\text{cl}} = \{-\lambda_1, \dots, -\lambda_n, -\frac{1}{2}(d_i + d_j)\}$ is comprised of the

spectra of both blocks, where λ_i are eigenvalues of the Laplacian L and $i, j = 1, \dots, n$ with $i \neq j$. The generator \mathcal{L}^{qm} of the quantum walk ($\omega = 1$) has a purely imaginary spectrum. Since \mathcal{L}^{qm} is essentially the commutator between A and ρ the eigenvectors of \mathcal{L}^{qm} are of the form $|\alpha_i\rangle\langle\alpha_j|$. Here, $|\alpha_i\rangle$ with $i = 1, \dots, n$ are the eigenvectors with real eigenvalues α_i of the (real symmetric) adjacency matrix A . We obtain $\mathcal{L}^{\text{qm}}|\alpha_i\rangle\langle\alpha_j| = -i(\alpha_i - \alpha_j)|\alpha_i\rangle\langle\alpha_j|$ and the corresponding spectrum $\sigma^{\text{qm}} = \{i(\alpha_i - \alpha_j)\}$ with $i, j = 1, \dots, n$.

Generally, the ω -spectrum is a non-linear interpolation between σ^{cl} and σ^{qm} , parametrized by the coherence ω . While analytic expressions for σ^ω may be obtained for simple cases we show that the eigenvalues ν_i are finite and hence well defined for all values of ω . First note that the spectral radius $\varrho^\omega = \max_i |\nu_i|$ is bounded as $\varrho^\omega \leq \|\mathcal{L}^\omega\|$ for any matrix norm $\|\cdot\|$. From the properties of norms follows that $\|\mathcal{L}^\omega\| \leq \omega\|\mathcal{L}^{\text{qm}}\| + (1-\omega)\|\mathcal{L}^{\text{cl}}\|$, implying that the spectral radius ϱ^ω and hence all eigenvalues ν_i are indeed bounded by the finite expression $\|\mathcal{L}^{\text{qm}}\| + \|\mathcal{L}^{\text{cl}}\|$. For an explicit upper bound one can use the Frobenius norm, defined by $\|M\|^2 = \sum_i |\mu_i|^2$ for normal matrices M with eigenvalues μ_i . A more detailed characterization of σ^ω is provided in Ref. [44].

III. HIGHER DISTINGUISHING POWER FOR PARTIAL COHERENCE

It is clear from the previous analysis that the ω -spectrum for coherences $\omega = \{0, 1\}$ is fully determined by the A - and L -spectra, and the degrees d_i . Thus, the ω -spectrum has the same DIP as these invariants in the classical and fully coherent regimes; this is however not the case for intermediate coherence. The fundamental yet simple reason is that the spectrum of $\omega\mathcal{L}^{\text{qm}} + (1-\omega)\mathcal{L}^{\text{cl}}$ is not identical to $\omega\sigma^{\text{qm}} + (1-\omega)\sigma^{\text{cl}}$, except when \mathcal{L}^{qm} and \mathcal{L}^{cl} commute. Consequently, the ω -spectrum of two non-isomorphic graphs may be different even if they have identical traditional graph invariants, i.e., the degrees d_i and the spectra of A, L, \bar{A} and $|L|$. Conversely, two graphs for which the degrees d_i and the A - and L -spectra are different always have different ω -spectra.

The higher DIP for partially coherent QSWs is demonstrated by non-isomorphic graphs with different ω -spectra, but indistinguishable by traditional invariants [40, 41]. The first example is provided by the pair of graphs in Fig. 2(a), cospectral with respect to traditional matrix representations. Figure 2(d) shows the clearly distinct ω -spectra of the graphs for intermediate coherence $\omega = 1/2$. Therefore, spectra of QSWs under the influence of decoherence allow us to distinguish more graphs than QSWs in the classical and fully coherent regimes. The next non-isomorphic pair in Fig. 2(b) consists of A -cospectral *regular* graphs, having identical degrees $d_i \equiv d$ for all vertices, for which the representations A, L, \bar{A} and $|L|$ are equivalent with regard to graph spectra [40]. Despite their high symmetry, the graphs have also clearly distinct ω -spectra, shown in Fig. 2(e).

As for standard spectral methods, the DIP of ω -spectra is limited for graphs with highly degenerate eigenvalues. Known examples are *strongly regular* graphs [38], whose adjacency

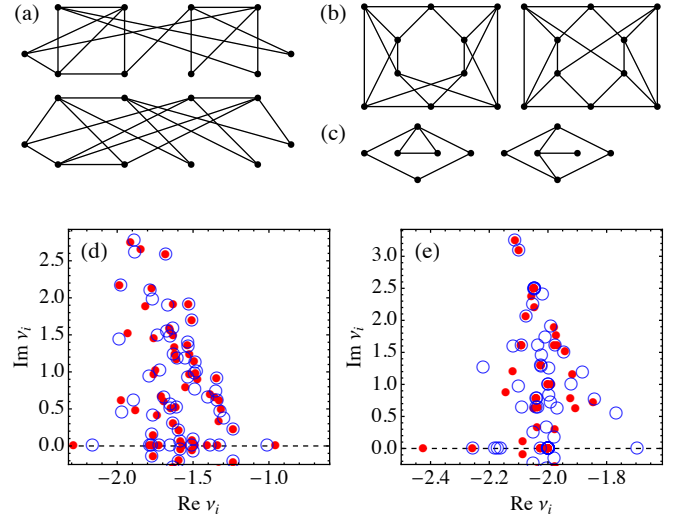


FIG. 2. Pairs of non-isomorphic graphs demonstrate the higher DIP of the ω -spectrum. The pairs in (a) and (b) are cospectral with respect to traditional matrix representations, but the corresponding ω -spectra in (d) and (e) are clearly distinct for intermediate coherence $\omega = 1/2$. The eigenvalues of the individual graphs (marked by \bullet and \circ) are distributed symmetrically about the real axis (dashed line). The pair of graphs in (c) is L -cospectral, but distinguishable by the ω -spectrum even in the classical regime $\omega = 0$.

matrix A has only three distinct eigenvalues for any number of vertices n . An example of a ω -cospectral pair of non-isomorphic strongly regular graphs are the Shrikhande graph and the lattice graph $L_2(4)$, having 16 vertices and identical ω -spectra with only 12 distinct eigenvalues. Several algorithms based on quantum walks are capable of distinguishing specific families of strongly regular graphs (see Ref. [26] for a comparison).

The DIP further reveals that classical random walks are not exactly equivalent to the classical limit of QSWs, generated by the Laplacian L and the dissipator \mathcal{L}^{cl} , respectively. The higher DIP of the ω -spectrum, compared to the L -spectrum, even persists in the classical regime $\omega = 0$ because of its dependence on the degrees d_i . This is exemplified by the pair of graphs in Fig. 2(c) with different degrees d_i , which are L -cospectral but distinguishable by the ω -spectrum for $\omega = 0$.

An obvious question is how the DIP depends on the level decoherence. We quantify the difference between the spectra of two graphs by the distance measure $\delta = \sum_{i=1}^n (|\text{Re}(\nu_i) - \text{Re}(\nu'_i)| + |\text{Im}(\nu_i) - \text{Im}(\nu'_i)|)$, where real and imaginary parts of ν_i, ν'_i are ordered before comparison. Figure 3(a) shows the distance δ in dependence on the coherence ω for the graphs in Fig. 2. The ω -spectra differ significantly over a wide range of the quantum-to-classical transition and no specific level of coherence is required for distinguishing graphs. Interestingly, for the pairs in Fig. 2(a) and (b), the DIP is maximal approximately halfway through the transition, indicating that decoherence is essential for the performance of the algorithm.

The DIP of the ω -spectrum compared to traditional spectra is summarized in Fig. 3(b). Each class in the diagram consists of all non-isomorphic pairs of graphs that are distinguishable

by the spectrum of either A , L or \mathcal{L}^ω , as indicated. The important result is that the class of pairs distinguished by the ω -spectrum includes the entire classes defined by A and L , and additional pairs not in these classes. However, not all pairs are distinguishable by their ω -spectra, as exemplified by strongly regular graphs.

IV. CONSTRUCTING ω -SPECTRA FROM LOCAL FLUCTUATIONS

It is possible, in principle, to use the ω -spectrum as the basis for quantum-inspired algorithms. Such polynomial-time algorithms would involve the classical computation of the ω -spectra of two graphs and their subsequent comparison. However, we want to exploit the properties of QSWs in order to design a quantum algorithm that relies on direct observations of QSWs and performs optimally in the presence of decoherence. This is achieved by means of a counting device that monitors stochastic jumps of the QSW across an auxiliary edge. Information about the graph structure is then encoded in the counting statistics $p(N)$ of the number of jumps N per time interval. As an essential part of our algorithm, we now explain how to determine the ω -spectrum from the counting statistics $p(N)$.

The counting statistics is obtained from the measuring device, consisting of the auxiliary directed edge ($u \rightarrow v$) with weight ϵ , shown in Fig. 1. The vertices u and v are previously unconnected, that is $(u, v) \notin E$, but otherwise chosen arbitrarily. Similar to regular edges, the auxiliary edge is described by the dissipator

$$\mathcal{L}^{\text{aux}} \rho = \epsilon \left(\Upsilon_{uv} \rho \Upsilon_{uv}^\dagger - \frac{1}{2} \{ \Upsilon_{uv}^\dagger \Upsilon_{uv}, \rho \} \right). \quad (4)$$

The weight $\epsilon \ll 1$ is sufficiently small such that \mathcal{L}^{aux} results in a negligible perturbation of \mathcal{L}^ω and σ^ω . The device measures fluctuations of random trajectories of the QSW in the steady state ρ^{ss} , specified by $(\mathcal{L}^\omega + \mathcal{L}^{\text{aux}}) \rho^{\text{ss}} = 0$ for $\omega \in [0, 1]$. Fluctuations are manifest in the number of stochastic jumps N across the edge ($u \rightarrow v$) during a fixed time interval Δt . The random variable N , monitored by the device, is described by the counting statistics $p(N)$ or equivalently the cumulants $C_k = \partial^k g(\chi) / \partial \chi^k|_{\chi=0}$, with $g(\chi) = \log \mathbb{E}(e^{\chi N})$ the cumulant generating function.

The N -resolved density matrix ρ_N represents the QSW together with the counting device in state N . The Laplace transform $\rho_\chi = \sum_N \rho_N e^{\chi N}$ is governed by the non trace preserving master equation [35, 36]

$$\frac{d\rho_\chi(t)}{dt} = \mathcal{L}^\omega(\chi) \rho_\chi(t). \quad (5)$$

The generator $\mathcal{L}^\omega(\chi) = \mathcal{L}^\omega + \mathcal{L}^{\text{aux}}(\chi)$ depends on χ to account for the detector, where $\mathcal{L}^{\text{aux}}(\chi)$ is obtained from \mathcal{L}^{aux} through the substitution $\Upsilon_{uv} \rho \Upsilon_{uv}^\dagger \rightarrow e^\chi \Upsilon_{uv} \rho \Upsilon_{uv}^\dagger$. The cumulant generating function $g(\chi)$ is then found from the solution $\rho_\chi(t)$ of Eq. (5) in the long-time limit. Taking the trace over all states $|i\rangle$ yields $\mathbb{E}(e^{\chi N}) = \text{tr}[\rho_\chi(t)] \sim e^{g(\chi)t}$, with

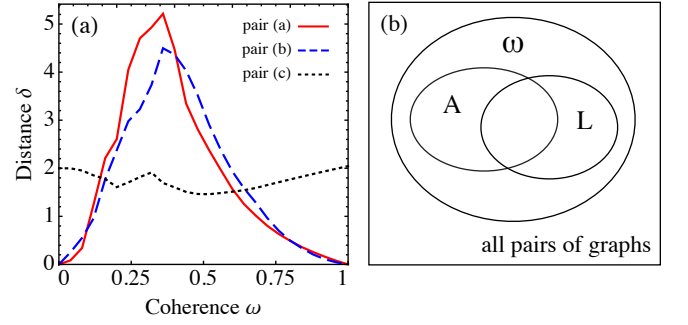


FIG. 3. (a) The distance δ between ω -spectra depending on the coherence ω for the pairs of graphs in Fig. 2. For pairs (a) and (b), the distance δ is peaked for intermediate coherence ω , whereas $\delta = 0$ in the classical and fully coherent limits. For the L -cospectral pair (c), the distance δ (rescaled) is always nonzero, even in the classical limit $\omega = 0$. (b) Pairs of graphs categorized into classes according to distinguishability with respect to different spectra. The class of pairs distinguishable by ω -spectra includes the classes defined by A - and L -spectra, and additional pairs not contained in these classes.

$\nu(\chi)$ the dominant eigenvalue of $\mathcal{L}^\omega(\chi)$, implying that $g(\chi) \sim \nu(\chi)t$ holds. Thus, for QSWs in the steady state, the reduced cumulants $c_k \equiv C_k / \Delta t$ are given by $c_k = \partial^k \nu(\chi) / \partial \chi^k|_{\chi=0}$.

Importantly, the cumulants c_k are directly related to the coefficients $q_i(\chi)$ of the characteristic polynomial $P^\omega(\nu, \chi) = \det[\nu \mathbb{1} - \mathcal{L}^\omega(\chi)]$. The equality $P^\omega[\nu(\chi), \chi] = 0$ holds by definition for any χ , such that by taking derivatives with respect to χ we obtain the infinite set of equations [45, 46]

$$\left. \frac{d^\ell P^\omega[\nu(\chi), \chi]}{d\chi^\ell} \right|_{\chi=0} = 0 \quad \ell = 1, 2, \dots \quad (6)$$

involving c_k , $q_i(\chi)$ and their derivatives. We reveal structural details of Eqs. (6) by taking derivatives of individual monomials $q_i(\chi) \nu^i(\chi)$ of the polynomial $P^\omega[\nu(\chi), \chi]$, yielding

$$\begin{aligned} & \frac{\partial^\ell}{\partial \chi^\ell} q_i(\chi) \nu^i(\chi) \Big|_{\chi=0} \\ &= \sum_{k=0}^{\ell} \sum_{|p|=k} \binom{\ell}{k} \binom{k}{p} \frac{\partial^{\ell-k}}{\partial \chi^{\ell-k}} q_i(\chi) \Big|_{\chi=0} c_{p_1} \cdots c_{p_i}, \end{aligned} \quad (7)$$

where $p = (p_1, \dots, p_i)$ is an i -tuple of positive integers and $|p| = p_1 + \dots + p_i$. The most important observation is that Eqs. (6) are linear in the coefficients $q_i(\chi)$. Further, all derivatives of $q_i(\chi)$ are identical to $q'_i(\chi)$ due to the factor e^χ and consequently Eqs. (6) depend on q_i and $q'_i \equiv q'_i(\chi)|_{\chi=0}$ only. Finally, because of the restriction $|p| = k$, we find that the ℓ -th equation depends on cumulants c_k with order $k \leq \ell$ and coefficients q_i, q'_i with indices $i \leq \ell$ and $i \leq \ell - 1$, respectively.

Equations (6) can be utilized to construct the ω -spectrum if sufficiently many cumulants c_k of the counting statistics $p(N)$ are known (see Ref. [45] for details). First note that Eqs. (6) involve $m = 2(n^2 - 1)$ independent coefficients q_1, \dots, q_{n^2-1} and q'_0, \dots, q'_{n^2-2} since $q_0 = q'_{n^2-1} = q'_{n^2} = 0$ and $q_{n^2} \equiv 1$. To determine the unknowns q_i, q'_i we set up a linear system

consisting of the first $\ell \leq m$ equations from (6), where cumulants c_k with order $k \leq m$ enter as numerical factors. The linear system has a unique solution for the coefficients q_i, q'_i , from which the characteristic polynomial $P^\omega(\nu)$ and the desired ω -spectrum are found. Note that the coefficients q_i and ω -spectra are independent of the edge $(u \rightarrow v)$. By contrast, the counting statistics $p(N)$, the cumulants c_k and the coefficients q'_i depend on the arbitrary choice of $(u \rightarrow v)$ and are therefore not suitable as graph invariants.

The cumulants c_k are in practice approximated by unbiased minimum-variance estimators \hat{c}_k obtained from s repeated observations of the number of jumps N occurring during the interval Δt [47]. According to the Cramér-Rao bound [48], their precision is quantified by the variance $\text{Var}(\hat{c}_k) \sim k!c_2^k/s$, that is $s \sim k!$ for a prescribed precision. The observation time (i.e. runtime) necessary for determining ω -spectra from cumulants of order $k \sim n^2$ therefore scales factorially with n , and there is no speed advantage gained by the algorithm compared to conventional GI testing [16, 39]. Measuring cumulants with high precision seems challenging; however, this limitation might be overcome by introducing several auxiliary edges.

V. CONCLUSIONS

We have presented a quantum algorithm for graph isomorphism (GI) testing that is resilient to decoherence and performs optimal halfway through the quantum-to-classical tran-

sition. Specifically, local observations of partially coherent quantum stochastic walks (QSWs) on graphs make it possible to distinguish a large class of non-isomorphic graphs by means of their ω -spectra. While decoherence indeed improves the performance of our algorithm when compared to traditional graph spectra we still have to clarify how powerful ω -spectra are in comparison to other algorithms by systematic benchmarking with larger sets of graphs [27].

Aside from GI testing, the ω -spectrum contains further valuable information: The largest non-zero real part of the ω -spectrum determines the mixing time required for QSWs to reach the steady state [49]. Moreover, the ω -spectrum is closely related to the algebraic connectivity of the graph, i.e., the smallest non-zero eigenvalue of the Laplacian [50]. For graphs of moderate size it is even practical to reconstruct the full graph from the spectrum by using standard optimizations methods [51].

The presented methods for obtaining ω -spectra are applicable to classical random walks and, more generally, to open quantum systems [45]. With this flexibility, we hope that insights into quantum walks provided by our algorithm are transferable to other algorithmic problems as well as to physical and biological settings in which coherence plays an essential role.

ACKNOWLEDGMENTS

The authors acknowledge useful discussions with O. Marty, N. Killoran and A. Smirne. This work has been supported by an Alexander von Humboldt Professorship, the ERC Synergy grant BioQ and the EU projects SIQS and DIADEMS.

-
- [1] C. H. Bennett and D. P. DiVincenzo, “Quantum information and computation,” *Nature* **404**, 247 (2000).
 - [2] M. B. Plenio, S. F. Huelga, A. Beige, and P. L. Knight, “Cavity-loss-induced generation of entangled atoms,” *Phys. Rev. A* **59**, 2468 (1999).
 - [3] M. B. Plenio and S. F. Huelga, “Entangled light from white noise,” *Phys. Rev. Lett.* **88**, 197901 (2002).
 - [4] L. D. Contreras-Pulido and R. Aguado, “Entanglement between charge qubits induced by a common dissipative environment,” *Phys. Rev. B* **77**, 155420 (2008).
 - [5] S. Bose, P. L. Knight, M. B. Plenio, and V. Vedral, “Proposal for teleportation of an atomic state via cavity decay,” *Phys. Rev. Lett.* **83**, 5158 (1999).
 - [6] M. B. Plenio and S. F. Huelga, “Dephasing-assisted transport: quantum networks and biomolecules,” *New J. Phys.* **10**, 113019 (2008).
 - [7] M. Mohseni, P. Rebentrost, S. Lloyd, and A. Aspuru-Guzik, “Environment-assisted quantum walks in photosynthetic energy transfer,” *J. Chem. Phys.* **129**, 174106 (2008).
 - [8] F. Caruso, A. Crespi, A. G. Ciriolo, F. Sciarrino, and R. Oselame, “Fast escape from quantum mazes in integrated photonics,” Preprint arXiv:1501.06438 (2015).
 - [9] J. J. Mendoza-Arenas, T. Grujic, D. Jaksch, and S. R. Clark, “Dephasing enhanced transport in nonequilibrium strongly correlated quantum systems,” *Phys. Rev. B* **87**, 235130 (2013).
 - [10] L. D. Contreras-Pulido, M. Bruderer, S. F. Huelga, and M. B. Plenio, “Dephasing-assisted transport in linear triple quantum dots,” *New J. Phys.* **16**, 113061 (2014).
 - [11] M. Mosca, “Quantum algorithms,” in *Encyclopedia of Complexity and Systems Science* (Springer, 2009) p. 7088.
 - [12] A. M. Childs and W. Van Dam, “Quantum algorithms for algebraic problems,” *Rev. Mod. Phys.* **82**, 1 (2010).
 - [13] V. Kendon and B. Tregenna, “Decoherence can be useful in quantum walks,” *Phys. Rev. A* **67**, 042315 (2003).
 - [14] V. Kendon, “Decoherence in quantum walks—a review,” *Math. Structures Comput. Sci.* **17**, 1169 (2007).
 - [15] J. Köbler, U. Schöningh, and J. Torán, *The Graph Isomorphism Problem: Its Structural Complexity* (Birkhäuser Verlag, Basel, 1993).
 - [16] B. D. McKay and A. Piperno, “Practical graph isomorphism, II,” *J. Symb. Comput.* **60**, 94 (2014).
 - [17] L. Babai, “Graph isomorphism in quasipolynomial time,” in *Proceedings of the 48th Annual ACM SIGACT Symposium on Theory of Computing*, STOC 2016 (New York, NY, USA, 2016) p. 684.
 - [18] J. D. Whitfield, C. A. Rodríguez-Rosario, and A. Aspuru-Guzik, “Quantum stochastic walks: A generalization of classical random walks and quantum walks,” *Phys. Rev. A* **81**, 022323 (2010).
 - [19] T. Rudolph, “Constructing physically intuitive graph invariants,” Preprint arXiv:quant-ph/0206068 (2002).

- [20] S.-Y. Shiao, R. Joynt, and S. N. Coppersmith, “Physically-motivated dynamical algorithms for the graph isomorphism problem,” *Quantum Inform. Comput.* **5**, 492 (2005).
- [21] B. L. Douglas and J. B. Wang, “A classical approach to the graph isomorphism problem using quantum walks,” *J. Phys. A: Math. Theor.* **41**, 075303 (2008).
- [22] J. K. Gamble, M. Friesen, D. Zhou, R. Joynt, and S. N. Coppersmith, “Two-particle quantum walks applied to the graph isomorphism problem,” *Phys. Rev. A* **81**, 052313 (2010).
- [23] S. D. Berry and J. B. Wang, “Two-particle quantum walks: Entanglement and graph isomorphism testing,” *Phys. Rev. A* **83**, 042317 (2011).
- [24] K. Rudinger, J. K. Gamble, M. Wellons, E. Bach, M. Friesen, R. Joynt, and S. N. Coppersmith, “Noninteracting multiparticle quantum random walks applied to the graph isomorphism problem for strongly regular graphs,” *Phys. Rev. A* **86**, 022334 (2012).
- [25] K. Rudinger, J. K. Gamble, E. Bach, M. Friesen, R. Joynt, and S. N. Coppersmith, “Comparing algorithms for graph isomorphism using discrete-and continuous-time quantum random walks,” *J. Comput. Theor. Nanosci.* **10**, 1653 (2013).
- [26] A. Mahasinghe, J. A. Izaac, J. B. Wang, and J. K. Wijerathne, “Phase-modified CTQW unable to distinguish strongly regular graphs efficiently,” *J. Phys. A: Math. Theor.* **48**, 265301 (2015).
- [27] D. Emms, S. Severini, R. C. Wilson, and E. R. Hancock, “Coined quantum walks lift the cospectrality of graphs and trees,” *Pattern Recognit.* **42**, 1988 (2009).
- [28] D. Tamascelli and L. Zanetti, “A quantum-walk-inspired adiabatic algorithm for solving graph isomorphism problems,” *J. Phys. A: Math. Theor.* **47**, 325302 (2014).
- [29] C. A. Ryan, M. Laforest, J. C. Boileau, and R. Laflamme, “Experimental implementation of a discrete-time quantum random walk on an NMR quantum-information processor,” *Phys. Rev. A* **72**, 062317 (2005).
- [30] H. Schmitz, R. Matjeschk, Ch. Schneider, J. Glueckert, M. Enderlein, T. Huber, and T. Schaetz, “Quantum walk of a trapped ion in phase space,” *Phys. Rev. Lett.* **103**, 090504 (2009).
- [31] F. Zähringer, G. Kirchmair, R. Gerritsma, E. Solano, R. Blatt, and C. F. Roos, “Realization of a quantum walk with one and two trapped ions,” *Phys. Rev. Lett.* **104**, 100503 (2010).
- [32] H. B. Perets, Y. Lahini, F. Pozzi, M. Sorel, R. Morandotti, and Y. Silberberg, “Realization of quantum walks with negligible decoherence in waveguide lattices,” *Phys. Rev. Lett.* **100**, 170506 (2008).
- [33] A. Schreiber, K. N. Cassemiro, V. Potoček, A. Gábris, P. J. Mosley, E. Andersson, I. Jex, and Ch. Silberhorn, “Photons walking the line: A quantum walk with adjustable coin operations,” *Phys. Rev. Lett.* **104**, 050502 (2010).
- [34] A. Aspuru-Guzik and P. Walther, “Photonic quantum simulators,” *Nat. Phys.* **8**, 285 (2012).
- [35] J. P. Garrahan and I. Lesanovsky, “Thermodynamics of quantum jump trajectories,” *Phys. Rev. Lett.* **104**, 160601 (2010).
- [36] G. Schaller, *Open Quantum Systems Far from Equilibrium*, Vol. 881 (Springer, 2014).
- [37] D. M. Cvetkovic, M. Doob, and H. Sachs, *Spectra of Graphs: Theory and Application* (Academic Press, New York, 1980).
- [38] A. E. Brouwer and W. H. Haemers, *Spectra of Graphs* (Springer Science & Business Media, 2011).
- [39] D. G. Corneil and D. G. Kirkpatrick, “A theoretical analysis of various heuristics for the graph isomorphism problem,” *SIAM J. Comput.* **9**, 281 (1980).
- [40] E. R. Van Dam and W. H. Haemers, “Which graphs are determined by their spectrum?” *Linear Algebra Appl.* **373**, 241 (2003).
- [41] W. H. Haemers and E. Spence, “Enumeration of cospectral graphs,” *European J. Combin.* **25**, 199 (2004).
- [42] R. C. Wilson and P. Zhu, “A study of graph spectra for comparing graphs and trees,” *Pattern Recognit.* **41**, 2833 (2008).
- [43] I. Mirzaev and J. Gunawardena, “Laplacian dynamics on general graphs,” *Bull. Math. Biol.* **75**, 2118–2149 (2013).
- [44] H. Wielandt, “On eigenvalues of sums of normal matrices,” *Pacific J. Math.* **5**, 633 (1955).
- [45] M. Bruderer, L. D. Contreras-Pulido, M. Thaller, L. Sironi, D. Obreschkow, and M. B. Plenio, “Inverse counting statistics for stochastic and open quantum systems: the characteristic polynomial approach,” *New J. Phys.* **16**, 033030 (2014).
- [46] A. Wachtel, J. Vollmer, and B. Altaner, “Fluctuating currents in stochastic thermodynamics. I. Gauge invariance of asymptotic statistics,” *Phys. Rev. E* **92**, 042132 (2015).
- [47] M. G. Kendall, *The Advanced Theory of Statistics*. (Charles Griffin and Co., Ltd., London, 1946).
- [48] S. Prasad and N. C. Menicucci, “Fisher information with respect to cumulants,” *IEEE Trans. Inform. Theory* **50**, 638 (2004).
- [49] O. Mülken and A. Blumen, “Continuous-time quantum walks: Models for coherent transport on complex networks,” *Phys. Rep.* **502**, 37 (2011).
- [50] M. Fiedler, “Algebraic connectivity of graphs,” *Czech. Math. J.* **23**, 298 (1973).
- [51] F. Comellas and J. Diaz-Lopez, “Spectral reconstruction of complex networks,” *Physica A* **387**, 6436 (2008).